Effects of Heat Treatment Conditions on the Thermal Properties of Mesophase Pitch-Derived Graphitic Foams

James W. Klett, April D. McMillan, Nidia C. Gallego, Timothy D. Burchell, Claudia A. Walls

Metals and Ceramics Division, Oak Ridge National Laboratory, Oak Ridge, TN, 37831

Carbon foam was first developed by researchers in the late 1960's as reticulated vitreous (glassy) carbon foams [1, 2]. More recently, Klett et. al. [3-5] at the Oak Ridge National Laboratory reported the first graphitic foams with bulk thermal conductivities greater than 58 W/m·K; thermal conductivities up to 180 W/m·K have recently been reported [6-8]. By combining an open cellular structure with a thermal conductivity to weight ratio (λ/ρ) greater than 200 (as compared to 45 for copper), the development of high conductivity graphitic foam presents a unique opportunity to radically change the approach to many heat transfer problems. For many graphitic materials, the heating rate during graphitization is critical to optimizing the material properties. Therefore, in this project we examine the influence of heating rate during graphitization on key properties of the foam, such as density, thermal diffusivity, and crystallinity.

Several billets of foam (~15 cm x ~10 cm x ~2.5 cm) were produced from Mitsubishi AR mesophase pitch powder with a softening point of 235°C. The mesophase pitch was foamed under 1000 psi pressure in aluminum pans utilizing two heating rates during (3.5 and 10°C/min foaming rate) [9]. The foaming step consisted of heating under vacuum to 250°C and soaking for 1 hour, applying the foaming pressure, and then heating at the specified heating rate to 600°C, soaking for one hour, and then cooling to room temperature (while simultaneously reducing pressure) at approximately 1.25 °C/min. All billets were marked for their position in

the furnace (i.e. bottom or top of furnace) and then carbonized to 1000°C under an atmospheric nitrogen purge at a heating rate of 0.2°C/min. The carbonized billets were then cut into 1.59 cm cubes in a regular pattern throughout the foam billets and the Euclidian density was measured for each cube (ASTM C559). The foam cubes were separated into four different groups for each initial foaming rate (3.5 and 10 °C/min) and subsequently heated to a graphitization temperature of 2800°C in four separate runs with different heating rates (1, 5, 10, and 15 °C/min) under an argon purge. Key material properties such as crystallographic structure, thermal diffusivity (measured by ASTM C714) and density were determined.

Table I reports the density uniformity for the billets processed under different foaming rates and in different positions within the furnace. As can be seen, there is little effect on uniformity (smaller deviations between the maximum and minimum values) due to the heating rate during foaming. However, a significant effect on density uniformity with the position in the furnace was observed. While there appeared to be some effect on density uniformity due to the foaming rate, this effect was small compared to the effect of the position of the pan in the furnace. It is known that a temperature gradient within the furnace exists as the exit path for off-gasses is at the top of the furnace. Hence, buoyancy effects cause the gasses from the bottom pan to rise and pass the upper pans on the way out, thus increasing their temperature. Perhaps, like steaming food, the gasses rising through the furnace result in much more uniform temperatures within the billets at the top of the furnace. Since the billet at the bottom does not get this effect, it may still contain large temperature non-uniformities during the foaming process, thus results in non-uniform foam.

The interlayer spacing (d_{002}), crystal stacking height ($Lc_{,002}$), and the crystal coherence length (or crystallite size) ($La_{,100}$) are indicators of crystalline perfection, and thus might be

expected to improve with lower heating rates since the elimination of defects is temperature and time dependent. Figure 1 shows the effect of heating rate on these parameters. It is seen that the d-spacing for all the samples (all heating rates) was between 0.3358 and 0.3368 nm and similar to that witnessed in previous studies with the foam [5]. However, there does not appear to be a correlation between either d_{002} or L_c with foaming rate, position in furnace, or graphitization rate. However, $L_{a,100}$ does show a strong correlation with foaming rate, position in furnace, and graphitization rate.

The thermal properties of the samples were then measured in all three directions (z, y, x). The z-direction is the vertical orientation of the billet and corresponds to the foaming direction. It is important to note here the mechanisms of pore formation. During foaming, the mesophase pitch is molten and begins to decompose. The decomposition gasses rise to the surface (bubble percolation) where they coalesce into larger bubbles and eventually rupture, like boiling water. This boiling action causes some orientation in the mesophase crystals, resulting in a preferred orientation of the a-direction of the crystals in this bubbling direction (z-direction). However, the decomposition of the pitch causes polymerization and increases its viscosity, thus impeding the flow of the bubbles to the surface. As the balance between decomposition and viscosity increase reaches a temperature unique to each pitch, the bubbles no longer flow to the surface, but rather simply form and enlarge, resulting in further alignment of the crystals along the cell walls due to biaxial extension. The foaming action is restrained by the container (and gravity), thus yielding a slight elongation of the bubbles in the z-direction. This elongation, along with the effect of the preferred orientation of the crystallites, results in a higher thermal conductivity in the z-direction than in the x-y direction.

Figure 2 shows the relationship of heating rate during graphitization on the x, y, and z thermal conductivities. From the plots, it is clear that the z-direction thermal conductivity is directly related to the graphitization heating rate. As anticipated in the previous section, the higher graphitization rate affects the crystal structure, thus decreasing the thermal conductivity in the direction with the greatest preferred orientation (z-direction). However, it is unclear why the x-direction thermal conductivity increased with increasing graphitization rate. This phenomenon was not seen in the y-direction, and this was also only seen in the samples made at the bottom of the furnace, not the top.

Figure 3 shows the z-direction thermal conductivity versus coherence length, L_a, and, as expected, there is a general trend that as the coherence length increases, the thermal conductivity increases. Thus, processing parameters which affect the coherence length will directly affect the final thermal conductivity.

The effect on the final thermal properties of the location in the foaming furnace is also noteworthy. It is clear that in the Z-direction (the direction with the highest conductivity), both billets that were located in the top of the furnace exhibited the highest overall thermal conductivity, irrespective of foaming rate. Moreover, it is also evident that the foaming rate does affect the final thermal properties, with the lower foaming rates yielding graphitized foams exhibiting the higher thermal conductivities. While these trends are also true for the x and y directions, the effects are less noticeable than those in the z-direction.

Several conclusions may be drawn from this study. The foams produced at the lower position in foaming furnace have a less uniform density than those foamed in the upper position. Moreover, the foaming rate of the precursor pitch is critical with samples foamed at lower heating rates. It was also observed that the graphitization rate was critical to the thermal

properties and that higher heating rates tended to disrupt the crystal structure (specifically the coherence length) and hence decrease the thermal properties compared to slower heat rates. Finally, it was found that the position in the furnace, and the foaming rate, exhibited a larger effect on the thermal properties than the graphitization rate. Thus, it appears that temperature uniformities within the billet during foaming are the most critical aspect of the process. Because the foaming stage (when the pitch is fluid) is critical to the formation and orientation of the crystallites (similar to mesophase pitch fibers [10]), further studies should focus on the foaming stage to allow tailoring the foam properties to the final application.

References

1. Ford W. Method of Making Cellular Refractory Thermal Insulating Material. US Patent 3,121,050. 1964.
2. Googin J, Napier J, and Scrivner M. Method for Manufacturing Foam Carbon Products. US Patent 3,345,440. 1967.
3. Klett J. High Thermal Conductivity, Mesophase Pitch-Derived Carbon Foam. Extended Abstracts, Proceedings of the 1998 43rd International SAMPE Symposium and Exhibition, Part 1 (of 2), Anaheim, California, U.S.A., 1998;745-55.
4. Klett J. Pitch-Based Carbon Foam and Composites. US Patent 6,261,485. 2001.
5. Klett J, et al. High-Thermal-Conductivity, Mesophase-Pitch-Derived Carbon Foams: Effect of Precursor on Structure and Properties. Carbon 2000; 38 (7):953-73.
6. Klett J, Klett L, Burchell T, and Walls C. Graphitic Foam Thermal Management Materials for Electronic Packaging. Socitey of Automotive Engineers Technical Paper Series 2000; (00FCC-117)
7. Gallego N, Klett J, and McMillan A. Effects of Processing Conditions on Properties of Graphite Foams. Extended Abstracts, Proceedings of The International Conference on Carbon in 2002, Beijing, China, 2002.
8. Klett J, McMillan AD, and Stinton D. Modeling Geometric Effects on Heat Transfer with Graphite Foam. Extended Abstracts, The 26th Annual Conference on Ceramic, Metal, and Carbon Composites, Materials, and Structures, Cocoa Beach, Florida, 2002.
9. Klett J. Process for Making Carbon Foam. US Patent 6,033,506. 2000.
10. Edie DD and Stoner EG, The Effect of Microstructure and Shape on Carbon Fiber Properties, in J.D. Buckley,editor.Carbon-Carbon Materials and Composites, Noyes Publications

List of Figures

List of Tables

Table I. Density uniformity of billets

	Bottom Pan†		Top Pan†	
Foaming Rate	Average Density	Max Deviation*	Average Density	Max Deviation*
[°C/min]	[g/cm^3]	[%]	[g/cm^3]	[%]
3.5	0.474	10.6	0.448	3.7
10	0.434	13.1	0.430	3.8

* defined as 100*(maximum density –minimum density)/mean

† bottom pan was located at the bottom of the furnace and top pan was located at the top.

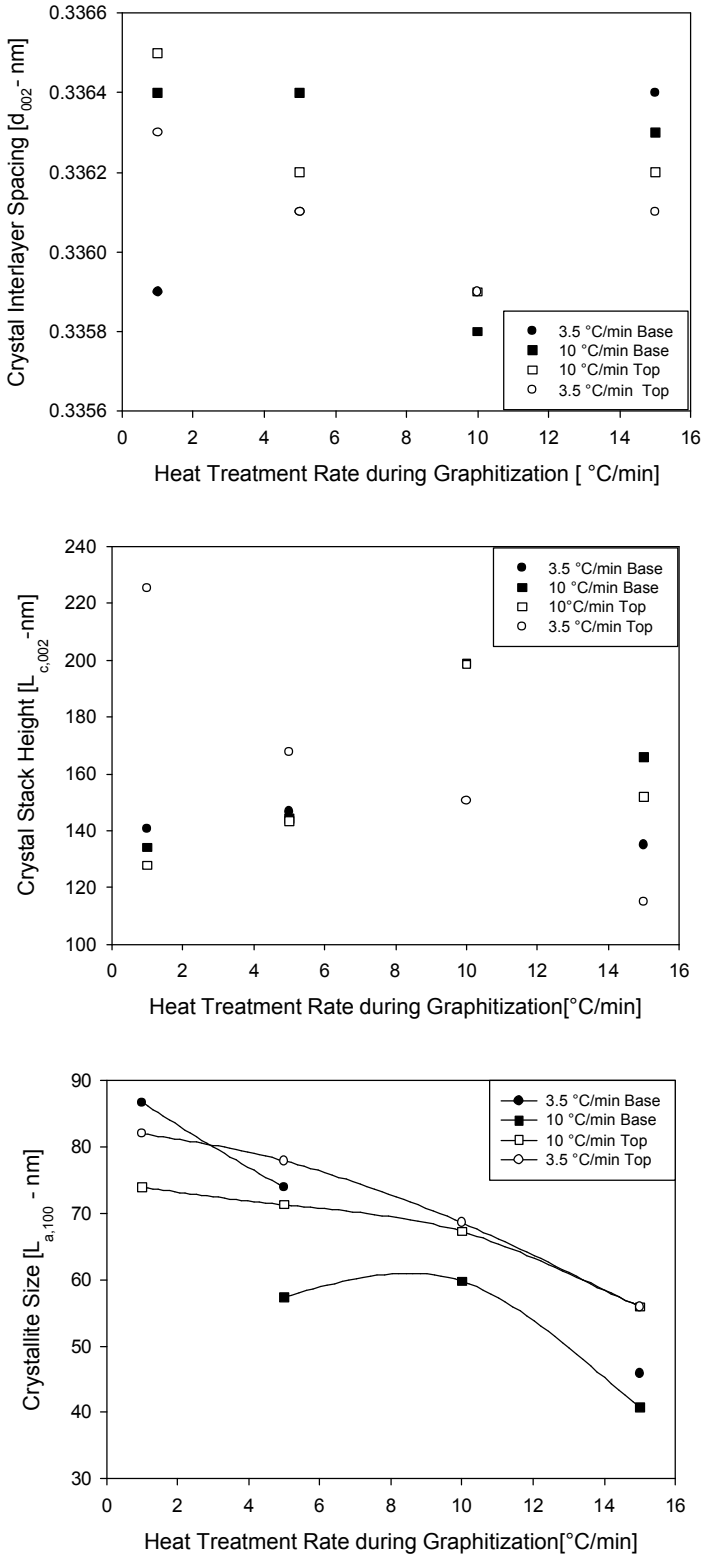

Figure 1. X-ray diffraction results - interlayer spacing-d_{002}, stacking height - L_c, coherence length - L_a.

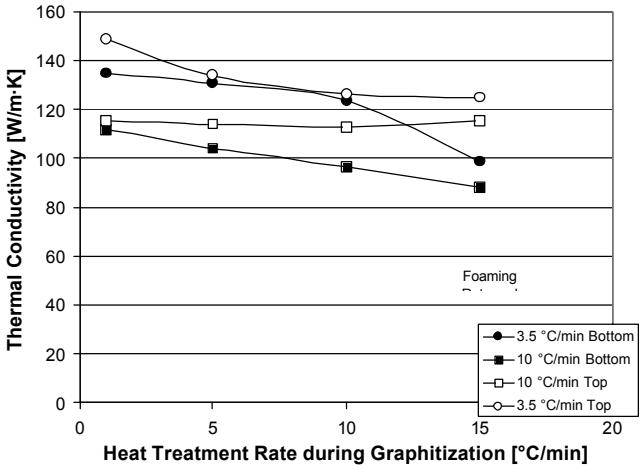

(a) Z-direction thermal conductivity

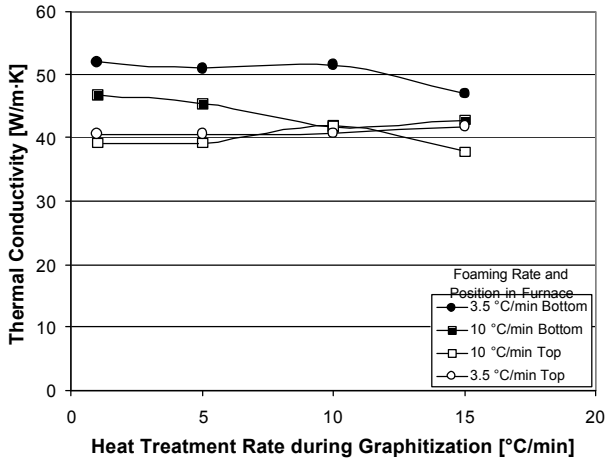

(b) Y-direction thermal conductivity

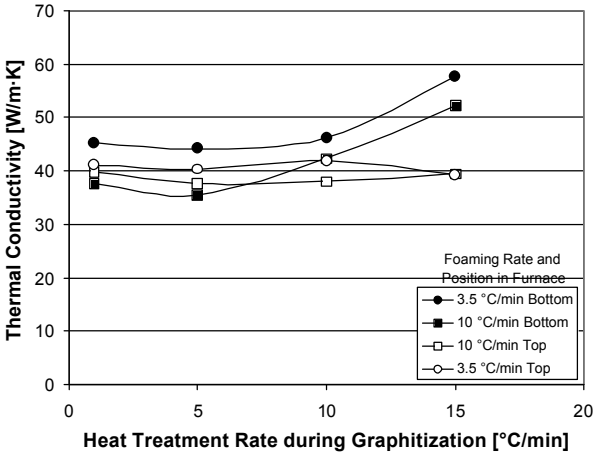

(c) X-direction thermal conductivity

Figure 2. Thermal conductivities in the (a) Z-direction, (b) Y-direction, (c) X-direction.

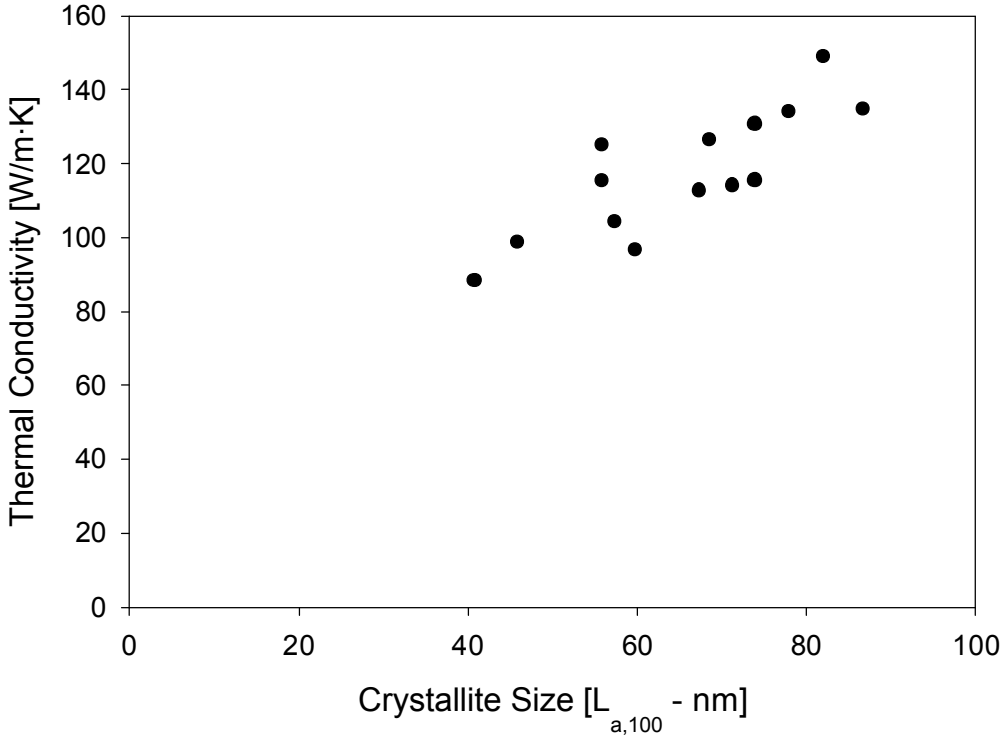

Figure 3. Z-direction thermal conductivity as a function of coherence length showing a strong dependence between the two parameters.